*Original Article*

DOI: 10.5582/bst.2012.v6.5.248

# Identification of MIWI-associated Poly(A) RNAs by immunoprecipitation with an anti-MIWI monoclonal antibody

**Takahiro Nishibu[1,2,*], Yukinobu Hayashida[1], Saori Tani[2], Sadamu Kurono[3,4], Kanako Kojima-Kita[5], Ryo Ukekawa[1], Tsutomu Kurokawa[1], Satomi Kuramochi-Miyagawa[6], Toru Nakano[5,6], Kunio Inoue[2], Susumu Honda[1]**

[1] *Life Science Research Laboratories, Wako Pure Chemical Industries Ltd., Hyogo, Japan;*
[2] *Graduate School of Science, Kobe University, Kobe, Japan;*
[3] *BMS Center, Wako Pure Chemical Industries Ltd., Osaka, Japan;*
[4] *Joint Research Laboratory of Molecular Signature Analysis, Graduate School of Medicine, Division of Health Sciences, Osaka University, Osaka, Japan;*
[5] *Graduate School of Frontier Biosciences, Osaka University, Osaka, Japan;*
[6] *Graduate School of Medical Sciences, Osaka University, Osaka, Japan.*

**Summary** **MIWI is one of the PIWI subfamily of proteins mainly expressed in mouse germ cells, and associates with pachytene piRNAs. MIWI has been thought to play an essential role in spermatogenesis and spermiogenesis *via* biogenesis and/or stability of pachytene piRNAs, retrotransposon silencing, and post-transcriptional regulation of target mRNAs. However, MIWI's detailed role and function are not well understood. In this study, we produced an anti-MIWI mouse monoclonal antibody and identified MIWI-associated poly(A) RNAs by immunoprecipitation from adult mouse testes lysates. Approximately 70% of the MIWI-associated poly(A) RNAs were known mRNAs and 30% of them were unknown non-coding RNAs. These poly(A) RNAs contained piRNA-encoding RNAs transcribed from piRNA cluster regions and piRNA-encoding mRNA, such as *Aym1* mRNA. Mature piRNAs specifically encoded in these piRNA-encoding RNAs were generated in pachytene spermatocytes and not detected in *Miwi*-deficient (*Miwi*$^{-/-}$) testes. Moreover, MIWI associated with a large number of known mRNAs whose expression levels were increased in pachytene spermatocytes, and the expression of these mRNAs was decreased in *Miwi*$^{-/-}$ testes at 20 days postpartum when pachytene spermatocytes were most abundant. These results strongly suggest that MIWI is involved in pachytene piRNA biogenesis and the positive regulation of target mRNA metabolism in pachytene spermatocytes *via* association with pachytene piRNA precursors and target mRNAs.**

***Keywords:*** MIWI, PIWI, piRNA, pachytene, spermatogenesis

## 1. Introduction

Argonaute family proteins, classified into AGO and PIWI subfamily proteins by amino acid sequence homology, play an important role in small RNA-mediated regulation of target gene expression. AGO subfamily proteins are ubiquitously expressed, whereas PIWI subfamily proteins are expressed mainly in germ cells (*1*). AGO subfamily proteins bind to microRNA (miRNA) or small interfering RNA of approximately 22 nucleotides in length, and function predominantly in post-transcriptional repression of target RNAs, *via* cleavage, translational repression and degradation mediated by the associated small RNA (*2-4*). On the other hand, PIWI subfamily proteins bind to PIWI-interacting RNAs (piRNAs) of approximately 25-31 nucleotides in length, but their functions have not been elucidated in detail (*5-9*).

There are three murine PIWI subfamily proteins, MIWI, MILI, and MIWI2. Each protein shows different

*Address correspondence to:
Dr. Takahiro Nishibu, Life Science Research Laboratories, Wako Pure Chemical Industries Ltd., 6-1 Takada-cho, Amagasaki, Hyogo 661-0963, Japan.
E-mail: nishibu.takahiro@wako-chem.co.jp

expression patterns during spermatogenesis. MIWI is expressed from meiotic pachytene spermatocytes to elongating spermatids, and *Miwi*-deficient (*Miwi*$^{-/-}$) mice display spermatogenic arrest at the round spermatid stage (*10*). MILI is expressed from primordial germ cells to round spermatids and MIWI2 is expressed in gonocytes (*11-14*). *Mili*$^{-/-}$ or *Miwi2*$^{-/-}$ mice display spermatogenic arrest between the early and mid- pachytene stage of meiosis (*11,12,14*). Thus, these three PIWI subfamily proteins are thought to play essential roles in spermatogenesis at different stages.

MILI and MIWI2 have been reported to associate with fetal piRNAs derived from repetitive retrotransposon genes in fetal gonocytes and to play an important role in gene silencing of retrotransposons *via* DNA methylation (*12,13,15,16*). Fetal piRNAs are generated from retrotransposon transcripts *via* the primary processing pathway and the secondary ping-pong amplification cycle pathway, and MILI and MIWI2 are directly involved in these pathways (*13*). In addition to MILI and MIWI2, other proteins, such as the TDRD family, MVH, GASZ, SUN1, and MOV10L1, are required for biogenesis of piRNAs and gene silencing of retrotransposons (*17-26*). These findings have begun to reveal the mechanisms of retrotransposon gene silencing mediated by MILI and MIWI2 in the primordial testis.

MIWI associates with pachytene piRNAs derived from various genomic regions that are unrelated to retrotransposons (*6,8*). The function of MIWI is therefore not thought to be limited to gene silencing of retrotransposons, although most recently MIWI has been reported to function in LINE1 retrotransposon silencing *via* its slicer activity (*27*). MIWI is concentrated in the chromatoid bodies, a germ cell-specific cytoplasmic structure that appears in the stages from pachytene spermatocytes to round spermatids. These chromatoid bodies contain RNA-processing proteins, such as Dicer, AGO2, and GW182. Therefore, MIWI is predicted to function in post-transcriptional control of target mRNAs (*28*). Certain mRNAs associated with MIWI are severely down-regulated in *Miwi*$^{-/-}$ mutants, suggesting that MIWI is required for target mRNA stability (*10*). As MIWI associates with mRNAs and piRNAs in the polysome fraction, MIWI is also thought to function in translational control of mRNAs (*29*). The detailed function of MIWI in post-transcriptional control of target mRNAs is unclear. In addition, MIWI has been reported to be required for the biogenesis and/or stability of pachytene piRNAs based on the result that pachytene piRNAs are not detected in *Miwi*$^{-/-}$ mutants (*7*). However, the function of MIWI in pachytene piRNA biogenesis is also still unknown.

AGO2, one of the AGO subfamily members, is a component of the chromatoid body similar to MIWI and plays an important role in post-transcriptional regulation of target mRNA mediated by miRNA. However, since spermatogenesis is not arrested in conditional *Ago2*$^{-/-}$ testes, AGO2 is not thought to be essential for spermatogenesis (*30*).

In this study, we analyzed poly(A) RNA present in MIWI complexes obtained by immunoprecipitation of adult mouse testes lysates, and compared them to poly(A) RNAs present in AGO2 complexes to reveal the function of MIWI. Our results suggest that MIWI may play an important role in pachytene piRNA biogenesis and the positive regulation of target mRNAs in pachytene spermatocytes.

## 2. Materials and Methods

### 2.1. *Ethics Statement*

Animal experiments were approved by the Institutional Animal Care and Use Committee of Wako Pure Chemical Industries Ltd. (approval ID: 19-5, 20-4, and 20-12).

### 2.2. *Production of monoclonal antibodies*

To produce anti-HIWI/MIWI and anti-mouse AGO2 monoclonal antibodies, a HIWI N-terminal region peptide TGRARARARGRARGQETAQ-bovine thyroglobulin (BTG) conjugate and a mouse AGO2 N-terminal region peptide YSGAGPVLASPAPTTSPIP-BTG conjugate were respectively injected into BALB/c mice. The B lymphocytes derived from the immunized mice were fused with P3U1 myeloma cells (ATCC). The resulting hybridomas were screened by enzyme-linked immunosorbent assays and immunoprecipitation assays using lysates of HEK293T cells (ATCC) that expressed FLAG-tagged HIWI or FLAG-tagged mouse AGO2, and an anti-HIWI/MIWI monoclonal antibody (2C12) and anti-mouse AGO2 monoclonal antibody (3E7) were established. The 2C12 hybridoma and the 3E7 hybridoma were injected into the abdominal cavity of adult mice and the ascites fluid was collected. Each monoclonal antibody was purified from the ascites fluid by affinity purification using Protein A Sepharose (GE Healthcare, Milwaukee, WI, USA).

### 2.3. *Immunoprecipitation and RNA purification*

Adult mouse testes (approximately 50 mg) were homogenized in 1 mL of cell lysis buffer (20 mM Tris-HCl, pH 7.4, 2.5 mM $MgCl_2$, 200 mM NaCl, 0.05% NP40), and the cell lysate was cleared by centrifugation at 20,000 × g for 20 min at 4°C. After filtration of the cell lysate using a 0.45 μm filter, 20 μL of Protein G-coupled beads (Life Technologies) bound with 5 μg of 2C12, 3E7, or non-specific mouse IgG was added to the cell lysate and mixed by rotation for 3 h at 4°C. The beads were washed three times with 1 mL of cell lysis buffer, and the immunoprecipitated protein-RNA

complex was eluted with 0.5% SDS. RNA contained in the eluted immunoprecipitated complex was extracted with phenol/chloroform, and precipitated with ethanol and Ethachinmate (Nippon Gene). The RNA sample was resuspended in nuclease-free water.

Total RNA was extracted from mouse testes samples with ISOGEN (Nippon Gene) according to the manufacturer's instructions. The extracted RNA was treated with Turbo DNase (Life Technologies) for 30 min at 37°C. After an additional phenol/chloroform extraction, the RNA was precipitated with ethanol and Ethachinmate, and was resuspended in nuclease-free water.

2.4. *cDNA synthesis and cloning*

The RNA purified from each immunoprecipitated product derived from approximately 50 mg of adult mouse testes was used as a template for cDNA synthesis. cDNA synthesis and PCR amplification were performed using a Target mRNA Cloning Kit (Wako, Osaka, Japan) according to the manufacturer's instructions and reference (*31*). PCR-amplified cDNA fragments were subcloned into the pGEM-T easy vector (Promega), and sequenced using a BigDye Terminator Cycle Sequencing Kit (Life Technologies). The sequence of these cDNA clones was analyzed by BLAST searches of DDBJ (*http://blast.ddbj.ac.jp/*) and NCBI (*http://blast.ncbi.nlm.nih.gov*), BLAT searches of UCSC (*http://genome.ucsc.edu/*) and homology searches of piRNABank (*http://pirnabank.ibab.ac.in/*).

2.5. *Gel electrophoresis and Western blotting*

The immunoprecipitated protein derived from approximately 25 mg of adult mouse testes was applied to SDS-PAGE using a 7.5% polyacrylamide gel followed by staining with a silver staining kit (Wako, Osaka, Japan). Western blotting was performed using anti-mouse AGO2 mouse monoclonal antibody 2D4 (1:1,000; Wako) as the primary antibody and horseradish peroxidase (HRP)-conjugated anti-mouse IgG rabbit polyclonal antibody (1:5,000; Dako) as the secondary antibody, or anti-MIWI rabbit polyclonal antibody MIWI-C (*11*) (1:1,000) as the primary antibody and HRP-conjugated anti-rabbit IgG goat polyclonal antibody (1:2,000; Dako) as the secondary antibody. The immunopurified RNA derived from approximately 25 mg of adult mouse testes was applied to gel electrophoresis in 0.5× Tris-borate-EDTA (TBE) buffer using a 10% polyacrylamide TBE-urea gel followed by staining with Clear Stain Ag (Nippon Gene). The PCR-amplified product of the cDNA derived from the poly(A) RNA in each immunoprecipitation product was analyzed by capillary electrophoresis with a Bioanalyzer DNA 1000 kit and a Bioanalyzer 2100 system (Agilent Technologies).

2.6. *Mass spectrometric analysis*

The protein bands stained with the Silver Stain MS Kit (Wako, Osaka, Japan) were excised and destained with De-staining Soln reagent in the Silver Stain MS Kit. The destained gel bands were rinsed in 50% acetonitrile/100 mM ammonium bicarbonate, dehydrated with acetonitrile and dried in a SpeedVac Concentrator (Thermo Electron). For in-gel protein digestion, Trypsin Gold, Mass Spectrometry Grade (Promega, Madison, WI, USA), was applied to each gel piece, followed by incubation in 50 μL of 10% acetonitrile/40 mM ammonium bicarbonate, overnight at 37°C. The extracted tryptic peptide solutions were dried and dissolved in 10 μL of 0.1% trifluoroacetic acid. The peptide solution was analyzed with a nano liquid chromatography (LC, UltiMate 3000, Dionex)-electrospray ionization-ion trap-mass spectrometer (ESI-IT-MS, HCTultra, Bruker Daltonics) or a matrix-assisted laser desorption/ionization time-of-flight mass spectrometer (MALDI-TOF-MS, AXIMA-CFR Plus, Shimadzu/Kratos Analytical). The data were entered into the Peptide Mass Fingerprint or the MS/MS Ion Search in the Mascot Search (Matrix Science) for a NCBInr protein database search to characterize the protein.

2.7. *Microarray analysis*

Total RNA (0.1 μg) and immunopurified RNA (0.1 μg) were amplified and labeled using an Amino Allyl MessageAmp™ II aRNA Amplification Kit (Life Technologies) according to the manufacturer's instructions. The aRNA derived from the total RNA and the immunopurified RNA were labeled with Cy3 and Cy5, respectively. Each labeled aRNA (1 μg) was hybridized to a 3D-Gene® Mouse Oligo chip 25k (Toray Industries Inc.) at 37°C for 16 h and the DNA chip was washed and dried according to the manufacturer's protocols. The fluorescence intensities of each probe were detected using a ScanArray scanner (PerkinElmer). The tiff image was analyzed using GenePix Pro® 6.0 (MDS Analytical Technologies). The data were filtered to remove low-confidence measurements, and were normalized by subtraction with the mean intensity of the background signal determined by the 95% confidence intervals of all the blank spots' signal intensities. The raw data intensities greater than two standard deviations from the background signal intensity were considered valid. Detected signals for each gene were normalized using the global normalization method according to the manufacturer's instructions. The data are MIAME compliant and the raw data have been deposited into the GEO database (Accession number: GSE27582). The pathway analysis of mRNAs that were enriched in the MIWI-IP products and the AGO2-IP products was performed using GenMAPP pathway profiler (*http://www.genmapp.org/*).

2.8. *Quantitative PCR*

The whole sample of immunopurified RNA derived from approximately 50 mg of adult mouse testes, and 1 μg of total RNA derived from mouse testes samples were used as templates for reverse transcription, which was performed with a SuperScript VILO cDNA Synthesis Kit (Life Technologies) according to the manufacturer's instructions. Eight-fold and 40-fold diluted reverse transcription products derived from the immunopurified RNA and the total RNA, respectively, were used as a template for quantitative PCR, which was performed with gene-specific primer pairs and 2× Power SYBR Master Mix (Life Technologies) on an ABI 7500 real-time PCR system (Life Technologies) according to the manufacturer's instructions. The sequences of the primers are described in Table S1.

2.9. *Northern blotting*

Six micrograms of total RNA purified from each testes sample were separated on a 12% denaturing polyacrylamide gel and blotted onto a nylon membrane (Biodyne plus; Pall Corporation). The blots were prehybridized in hybridization buffer (50% formamide, 5× saline-sodium citrate (SSC), 2% blocking solution, 0.1% N-lauroyl sarcosine, 0.1% SDS, 200 μg/mL yeast tRNA) for 1 h at 60°C. LNA-modified DNA probes labeled with digoxigenin at the 5' end were added to the hybridization buffer and incubated with the blots overnight at 60°C. The nucleotide sequences of the LNA probes were for piR-108116, 5'-TAGGCGACTAAGTG TGTTGTGCAAAATGTA-3' and for U6 snRNA, 5'-A TCGTTCCAATTTTAGTATATGTGCTGCCG-3'. The concentrations of the probe used for piR-108116 and U6 snRNA were 0.1 nM and 0.05 nM, respectively. After hybridization, the blots were washed twice with 2× SSC containing 0.1% SDS and once with 1× SSC containing 0.1% SDS at room temperature for 15 min each, and with 0.2× SSC containing 0.1% SDS and 0.1× SSC containing 0.1% SDS at 65°C for 30 min each. After a brief wash with maleic acid buffer (0.15 M NaCl, 0.1 M maleic acid, pH 7.5), the blots were incubated in 1% blocking reagent (Roche) in maleic acid buffer for 30 min, washed twice in maleic acid buffer containing 0.3% Tween 20, washed briefly in AP buffer (0.1 M NaCl, 0.1 M Tris-HCl, pH 9.5), incubated with CSPD-star chemiluminescent substrate (Roche) and finally the luminescent signal was detected with an ImageQuant LAS4000 mini image analyzer (GE Healthcare).

## 3. Results

3.1. *Isolation of MIWI complexes by immunoprecipitation*

To isolate MIWI complexes by immunoprecipitation, we produced an anti-HIWI/MIWI monoclonal antibody (2C12). As an antigen, we used a HIWI N-terminal region peptide with high homology to MIWI and low homology to other PIWI subfamily proteins, and this region is outside of the PAZ domain that serves as binding site for small RNA (Figures S1A and S1B). To isolate AGO2 complexes to compare with MIWI complexes, we also produced an anti-mouse AGO2 monoclonal antibody (3E7) in a similar manner using a mouse AGO2 N-terminal region peptide whose sequence showed low homology to other AGO subfamily proteins, and this region is also outside of the PAZ domain (Figures S2A and S2B). Using these antibodies, we performed immunoprecipitation experiments with adult mouse testes. Western blotting with anti-MIWI rabbit polyclonal antibody (MIWI-C) and anti-mouse AGO2 mouse monoclonal antibody (2D4) showed that 2C12 and 3E7 immunoprecipitated MIWI and AGO2, respectively (Figure 1A). Mass spectrometric analysis showed multiple protein bands except for the AGO2-band detected in anti-AGO2-immunoprecipitated (AGO2-IP) products containing HSPA2 (heat shock protein 2) that is a family protein of heat shock protein 70 reported to associate with human AGO2 (*32*). However, the other co-precipitated proteins are unknown to associate with AGO2 (data not shown), and it is possible that these proteins were bound to 3E7 or AGO2 non-specifically. Two protein bands detected at around 90 to 100 kDa in anti-MIWI-immunoprecipitated (MIWI-IP) products by silver staining (Figure 1A) were identified as TUBGCP2 (tublin, gamma complex associated protein 2) (asterisk) and MIWI (double asterisks) by mass spectrometric analysis. Moreover, the other protein bands detected at around 70 kDa and 200 kDa in the MIWI-IP products were identified as HSPA2 and a hypothetical protein LOC230393, respectively (data not shown). Since the interaction of MIWI with TUBGCP2 was observed in transiently expressed HEK293T cells and in adult mouse testes (Figures S3A and S3B), MIWI is considered to specifically interact with TUBGCP2. When we substituted Empigen BB, a strong zwitterionic detergent, for immunoprecipitation in place of NP-40, silver staining detected a major protein band of MIWI and a minor protein band of HSPA2 considered as a chaperone protein, (Figure S4). These results showed that 2C12 specifically binds to MIWI.

Using denaturing polyacrylamide gel electrophoresis, we detected small RNAs of approximately 30 nucleotides in length in the MIWI-IP products, which corresponded to piRNAs. In contrast, we detected small RNAs of approximately 22 nucleotides in length, which corresponded to miRNAs, in AGO2-IP products (Figure 1B). We cloned the small RNAs in the MIWI-IP products and characterized 93 clones in detail. Twenty-five percent of these small RNAs showed no homology to known piRNAs but matched perfectly to genomic sequences while 72%

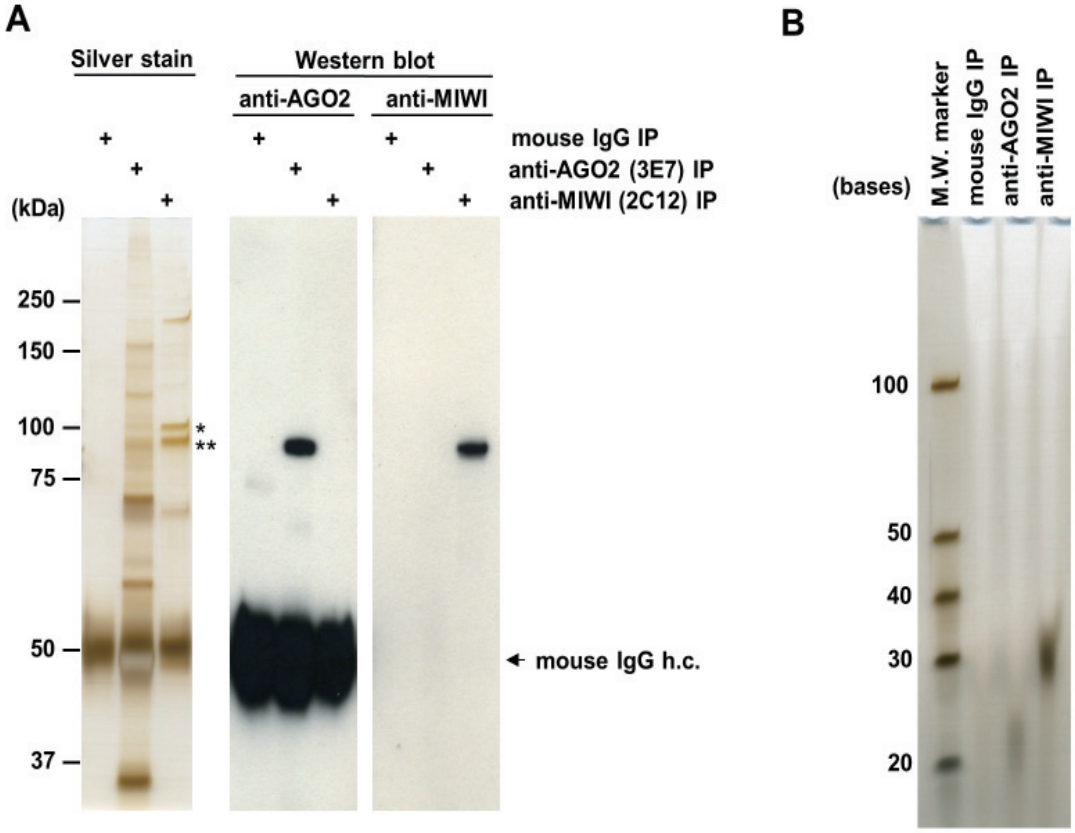


**Figure 1. Isolation of the MIWI complex by immunoprecipitation. (A)** Silver staining and Western blotting of immunoprecipitated (IP) proteins. The proteins immunoprecipitated from adult mouse testes using an anti-mouse AGO2 monoclonal antibody (3E7) or an anti-MIWI monoclonal antibody (2C12) were analyzed by SDS-polyacrylamide gel electrophoresis followed by silver staining (left panel), and Western blotting using an anti-mouse AGO2 mouse monoclonal antibody (2D4) (central panel) and an anti-MIWI rabbit polyclonal antibody (MIWI-C) (right panel). Immunoprecipitation with non-specific mouse IgG was performed as a negative control. Two silver stained protein bands of nearly 100 kDa in anti-MIWI-immunoprecipitated (MIWI-IP) products (left panel) were identified as TUBGCP2 (tublin, gamma complex associated protein 2) (asterisk) and MIWI (double asterisks) by mass spectrometric analysis. Silver stained protein bands of approximately 50 kDa (left panel) corresponded to the heavy chain (h.c.) of mouse IgG, which was detected by Western blotting using a HRP-conjugated anti-mouse IgG rabbit polyclonal antibody as the secondary antibody (central panel), but was not detected by Western blotting using a HRP-conjugated anti-rabbit IgG goat polyclonal antibody as the secondary antibody (right panel). **(B)** Silver staining of immunoprecipitated small RNAs. The small RNAs immunoprecipitated from adult mouse testes using 3E7 and 2C12 were analyzed by denaturing polyacrylamide gel electrophoresis followed by silver staining. Immunoprecipitation with non-specific mouse IgG was performed as a negative control. M.W., molecular weight.

showed substantial homology to known piRNAs (Figure S5A). The average length of the 93 clones was 30.1 ± 1.4 nucleotides, which corresponds to pachytene piRNAs (*6,7*), and only approximately 10% of these clones showed substantial homology to retrotransposon sequences in contrast to the fetal piRNAs and pre-pachytene piRNAs that include many sequences derived from retrotransposons (*12,13,15,16*). In the primary processing pathway of piRNA biogenesis, single-stranded piRNA precursor transcripts generate a diverse set of piRNA sequences that share a preference for uridine at the 5' end (1st U) (*5,6*). On the other hand, secondary piRNAs generated by the ping-pong amplification cycle have a strong preference for adenine at position 10 (10th A) (*13,33,34*). In this study approximately 80% of the 93 clones had a 1st U (Figure S5B), indicating that these clones encode piRNAs generated by the primary processing pathway. These results suggest that MIWI-associated small RNAs isolated from mouse adult testes by immunoprecipitation with 2C12 are pachytene piRNAs.

### 3.2. *Isolation of poly(A) RNAs contained in the MIWI-IP products*

We previously established a cDNA cloning method utilizing an adaptor ligation to identify poly(A) RNA in immunoprecipitated products, and succeeded in identifying target mRNA candidates of miRNAs in the AGO2-IP products of HeLa cells and HepG2 cells (*31*). In order to examine whether poly(A) RNAs are contained in the MIWI-IP and AGO2-IP products of adult mouse testes, we performed cDNA cloning of poly(A) RNAs in both products using the same method. We detected PCR amplification products in both IPs but did not detect any amplification from the control non-specific mouse IgG-immunoprecipitated (mouse IgG-IP) products (Figure 2A). Therefore, poly(A) RNAs

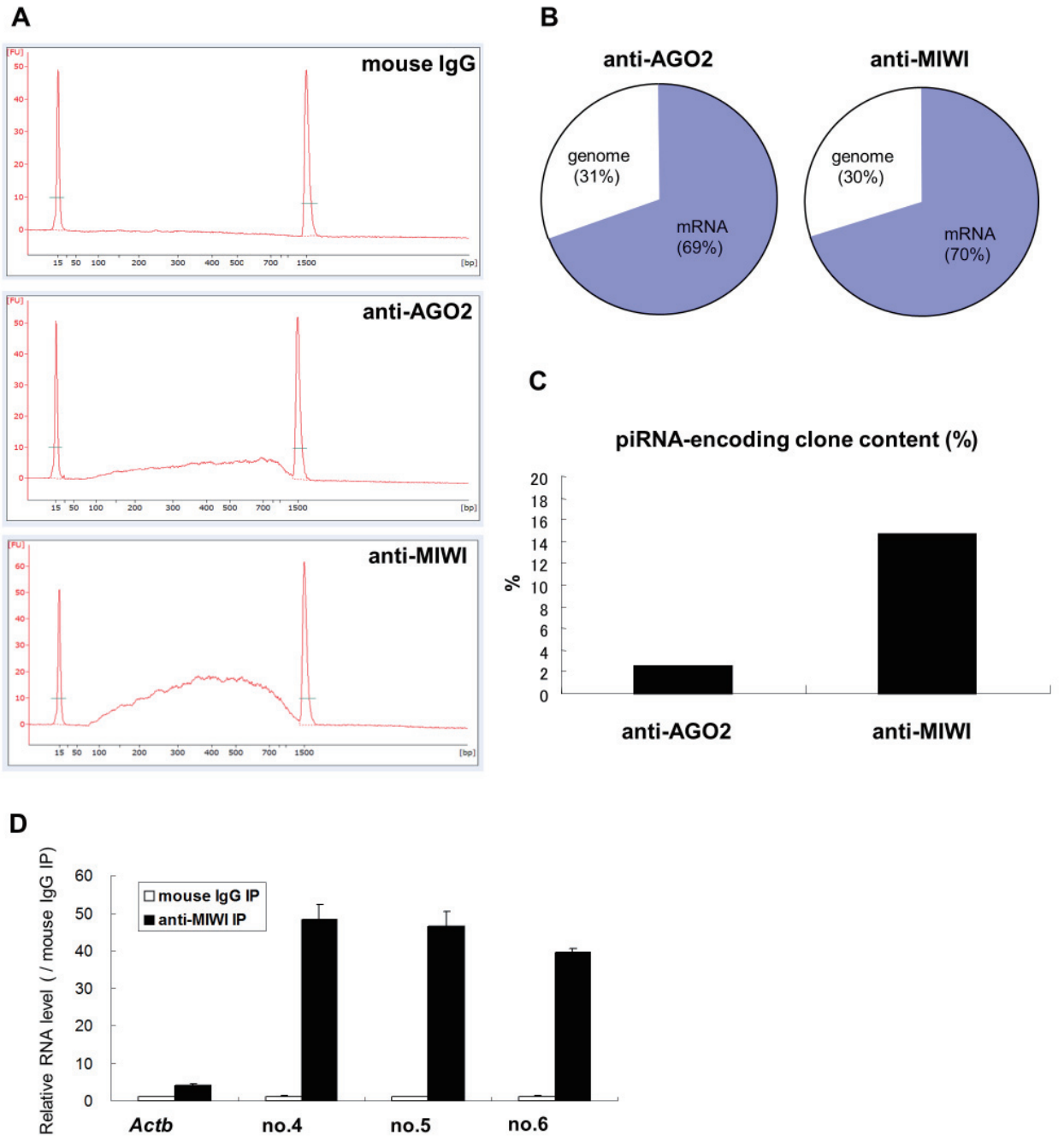


**Figure 2. cDNA cloning of poly(A) RNAs contained in the MIWI-IP products. (A)** Electropherograms of PCR-amplified cDNA products derived from IP poly(A) RNAs. The PCR products of cDNA derived from poly(A) RNAs that were immunoprecipitated from adult mouse testes with 3E7 and 2C12 were analyzed by capillary electrophoresis. The peaks at 15 bp and 1,500 bp correspond to the lower and upper markers, respectively. Immunoprecipitation with non-specific mouse IgG was performed as a negative control. **(B)** Composition of 278 cDNA clones derived from AGO2-IP poly(A) RNAs and 280 cDNA clones derived from MIWI-IP poly(A) RNAs. All cDNA clones were categorized as clones that matched mRNAs ("mRNA") or clones that showed no homology to known mRNAs but matched perfectly to the genomic sequence ("genome"). **(C)** Proportion of piRNA-encoding clones among the "genome" clones derived from AGO2-IP poly(A) RNAs and MIWI-IP poly(A) RNAs. **(D)** Enrichment levels of piRNA-encoding RNAs in the MIWI-IP products. The RNA levels of three piRNA-encoding RNAs (clone Nos. 4, 5 and 6) and *Actb* mRNA in mouse IgG-IP RNA and MIWI-IP RNA isolated from adult testes were analyzed by quantitative PCR and normalized to those of *Gapdh*. The normalized levels in MIWI-IP RNA were compared with those in mouse IgG-IP RNA.

were present in the MIWI-IP products as well as in the AGO2-IP products. We analyzed the sequence of 280 cDNA clones obtained from the MIWI-IP products and the 278 cDNA clones obtained from the AGO2-IP products. In both sets of IP products, approximately 70% of cDNA clones showed substantial homology to known mRNAs and the remainder showed no homology to known mRNAs, but matched perfectly to the genomic sequence (Figure 2B). These results indicated that mRNAs and non-coding poly(A) RNAs

are included in the MIWI complex as well as in the AGO2 complex.

### 3.3. *MIWI associates with piRNA-encoding RNAs*

We then focused on the cDNA clones that showed no homology to known mRNAs but matched perfectly to the genomic sequence. Since pachytene piRNAs associated with MIWI are exclusively produced by the primary processing pathway, we assumed that the piRNA precursor transcripts would be present in the MIWI-IP products and investigated by homology searching of databases whether the unknown non-coding clones represented piRNA-encoding sequences. We found that approximately 15% of the unknown non-coding clones derived from the MIWI-IP products represented piRNA-encoding sequences, whereas only approximately 2% of those derived from the AGO2-IP products did (Figure 2C). There were eight clones that encoded a single piRNA and four clones that encoded multiple piRNAs (Table 1). Clone Nos. 4 and 6 matched to the genomic sequence of the same piRNA cluster region on chromosome 7, and clone No. 5 matched to another piRNA cluster region on chromosome 7. We considered that these three piRNA-encoding clones might encode piRNA precursors transcribed from a piRNA cluster. These three piRNA-encoding RNAs were highly enriched in the MIWI-IP products compared to housekeeping *Actb* mRNA (Figure 2D). We cloned the 5' terminal region of clone No. 5 using rapid amplification of cDNA ends (RACE) and identified a 322 bp 5' terminal region. We identified 72 piRNA species within the 540 bp length of clone No. 5 and the 5' terminal nucleotide of 92% of the 72 piRNAs was uridine (data not shown). These results suggest that clone No. 5 is a pachytene piRNA precursor transcribed from the piRNA cluster region or an intermediate of a piRNA precursor generated by additional processing.

### 3.4. *A piRNA-encoding RNA associated with MIWI is a pachytene piRNA precursor*

We investigated the expression pattern of three piRNA-encoding RNAs (clone Nos. 4, 5 and 6) derived from chromosome 7 during spermatogenesis. In the mouse testis, pachytene spermatocytes are first found at 14 days postpartum (dpp) and the percentage of pachytene spermatocytes is highest at 18-20 dpp (*35*). The expression level of these three piRNA-encoding RNAs in mouse testes at 12-24 dpp was compared with the levels of Miwi and three known pachytene markers (*Ccna1* (*36*), *Dmrtc2* (*37*) and *Ovol1* (*38*)), and *Actb* mRNAs. The expression levels of the piRNA-encoding RNAs tended to increase from 12-20 dpp, similarly to those of *Miwi* and the pachytene marker mRNAs, whereas that of *Actb* mRNA were constant (Figure 3A). Furthermore, Northern blotting analysis showed that one of the piRNAs specifically encoded in clone No. 5, piR-108166, also increased from 12-20 dpp (Figure 3B). These results indicate that piRNA-encoding RNAs enriched in the MIWI-IP products are pachytene piRNA precursors or intermediates of such.

To clarify whether MIWI participates in piR-108166 biogenesis, we compared the RNA levels of the piRNA-encoding clone No. 5 and piR-108166 in *Miwi*$^{+/-}$ and *Miwi*$^{-/-}$ testes at 24 dpp. The RNA level of piR-108166 was undetectable in *Miwi*$^{-/-}$ testes (Figure 3C). In contrast, the RNA level of clone No. 5 did not show such a reduction in *Miwi*$^{-/-}$ testes (Figure 3D). These results suggest that MIWI is essential for biogenesis of pachytene piRNA and is involved in processing of precursor RNA.

### 3.5. *MIWI associates with mRNAs whose expression levels are increased in pachytene spermatocytes*

Next, we analyzed the protein-encoding mRNAs present in the AGO2-IP products and the MIWI-IP products comprehensively, by microarray analysis. We identified mRNAs enriched in the IP products by examining the ratio of the signal intensity in AGO2-IP RNA or MIWI-IP RNA to total RNA signal intensity. Based on an IP RNA/total RNA signal ratio ≥ 2.0, we selected 1,644 and 1,739 mRNAs that were enriched in the AGO2-IP and MIWI-IP products respectively, for further analysis (Figure 4A). Many different mRNAs

**Table 1. piRNA-encoding clones in the "genome" (non-mRNA-matching) clones derived from the MIWI-IP products**

| Clone No. | cDNA length | Chromosome (strand) | Number of encoded piRNA | piRNA cluster region |
|---|---|---|---|---|
| 1 | 158 base | ch.1 (+) | 1 | Not hit |
| 2 | 334 base | ch.2 (+) | 1 | Not hit |
| 3 | 189 base | ch.6 (+) | 2 | Not hit |
| 4 | 183 base | ch.7 (–) | 4 | Hit |
| 5 | 218 base | ch.7 (+) | 23 | Hit |
| 6 | 378 base | ch.7 (+) | 1 | Hit |
| 7 | 273 base | ch.8 (–) | 1 | Not hit |
| 8 | 273 base | ch.8 (–) | 1 | Not hit |
| 9 | 480 base | ch.9 (–) | 1 | Not hit |
| 10 | 271 base | ch.10 (–) | 1 | Not hit |
| 11 | 394 base | ch.14 (–) | 1 | Not hit |
| 12 | 61 base | ch.15 (–) | 3 | Not hit |

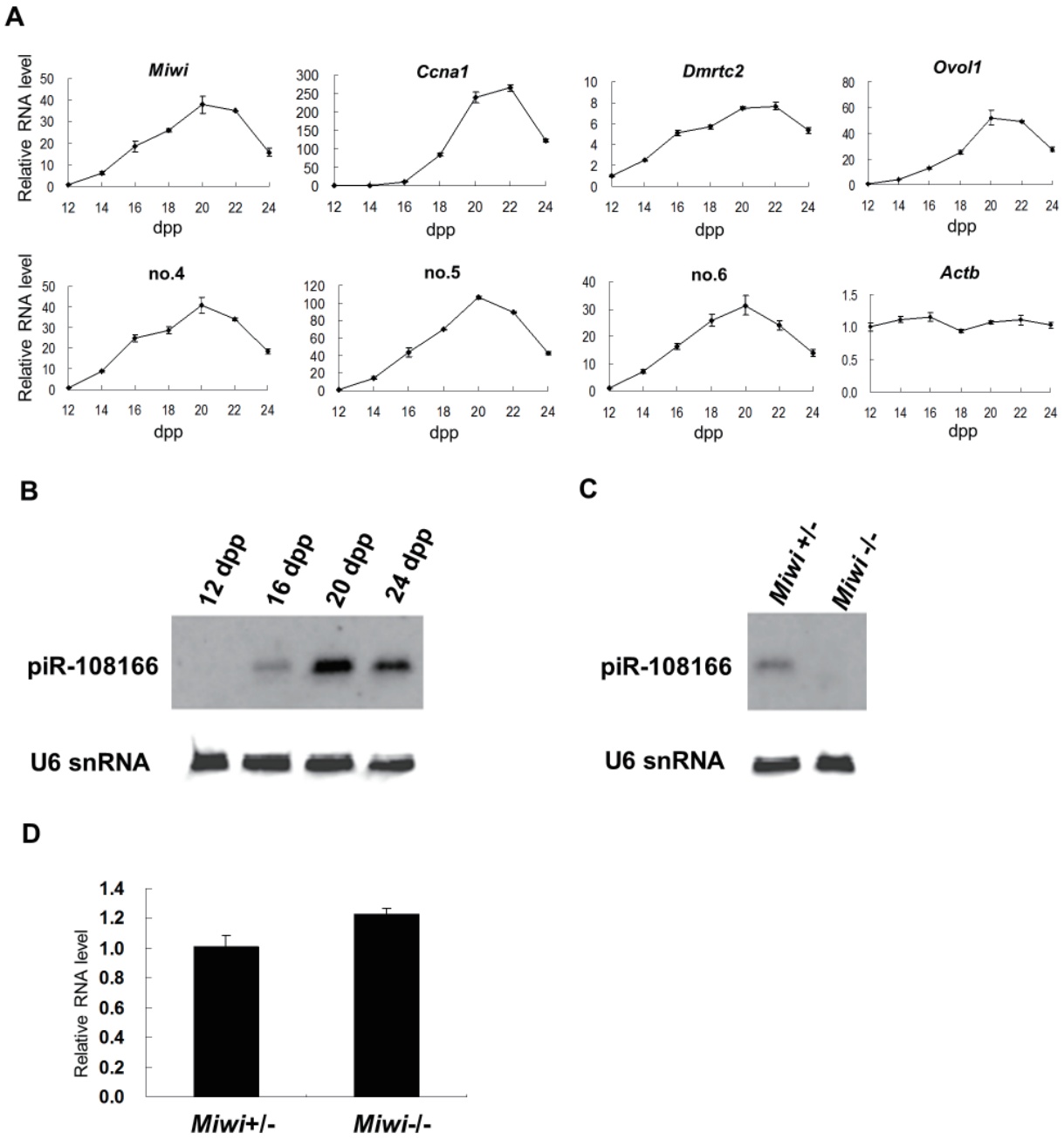


**Figure 3. Expression analysis of piRNA-encoding RNAs contained in the MIWI-IP products. (A)** Expression pattern of several piRNA-encoding RNAs contained in the MIWI-IP products during spermatogenesis. The expression levels of three piRNA-encoding RNAs (clone Nos. 4, 5 and 6) derived from chromosome 7, *Miwi* mRNA, three known pachytene marker mRNAs (*Ccna1*, *Dmrtc2*, *Ovol1*), and *Actb* mRNA in mouse testes at 12 to 24 days postpartum (dpp) were analyzed by quantitative PCR and normalized to those of *Gapdh*. The normalized levels were compared with those at 12 dpp. **(B)** Expression levels analyzed by Northern blotting of piR-108116, which was specifically encoded in piRNA-encoding RNA clone no. 5 during spermatogenesis in mouse testes at 12 to 24 dpp. **(C)** Comparison of RNA level of piR-108116 in *Miwi*$^{+/-}$ and *Miwi*$^{-/-}$ testes at 24 dpp by Northern blotting. **(D)** Comparison of the RNA levels of the piRNA-encoding RNA clone No. 5 in *Miwi*$^{+/-}$ and *Miwi*$^{-/-}$ testes at 24 dpp. The expression level of the piRNA-encoding RNA clone no. 5 was analyzed by quantitative PCR and normalized to that of Gapdh. The normalized level in *Miwi*$^{-/-}$ testes was compared to that in *Miwi*$^{+/-}$ testes.

were enriched in each group (Figure 4B). We selected the top ten mRNAs that were highly and specifically enriched in the AGO2-IP products (AGO2-IP/total RNA signal ratio ≥ 2.0 and MIWI-IP/total RNA signal ratio < 1.5) and MIWI-IP products (MIWI-IP/total RNA signal ratio ≥ 2.0 and AGO2-IP/total RNA signal ratio < 1.5), and investigated the expression level of these mRNAs in mouse testes at 12-24 dpp. We found that the mRNAs highly and specifically enriched in the MIWI-IP products were present at a higher level at 20 dpp compared to at 12 dpp (Table 2). However, the mRNAs highly and specifically enriched in the AGO2-IP products remained at nearly the same level. This result indicates that MIWI specifically associates with many mRNAs whose expression levels are increased in pachytene spermatocytes.

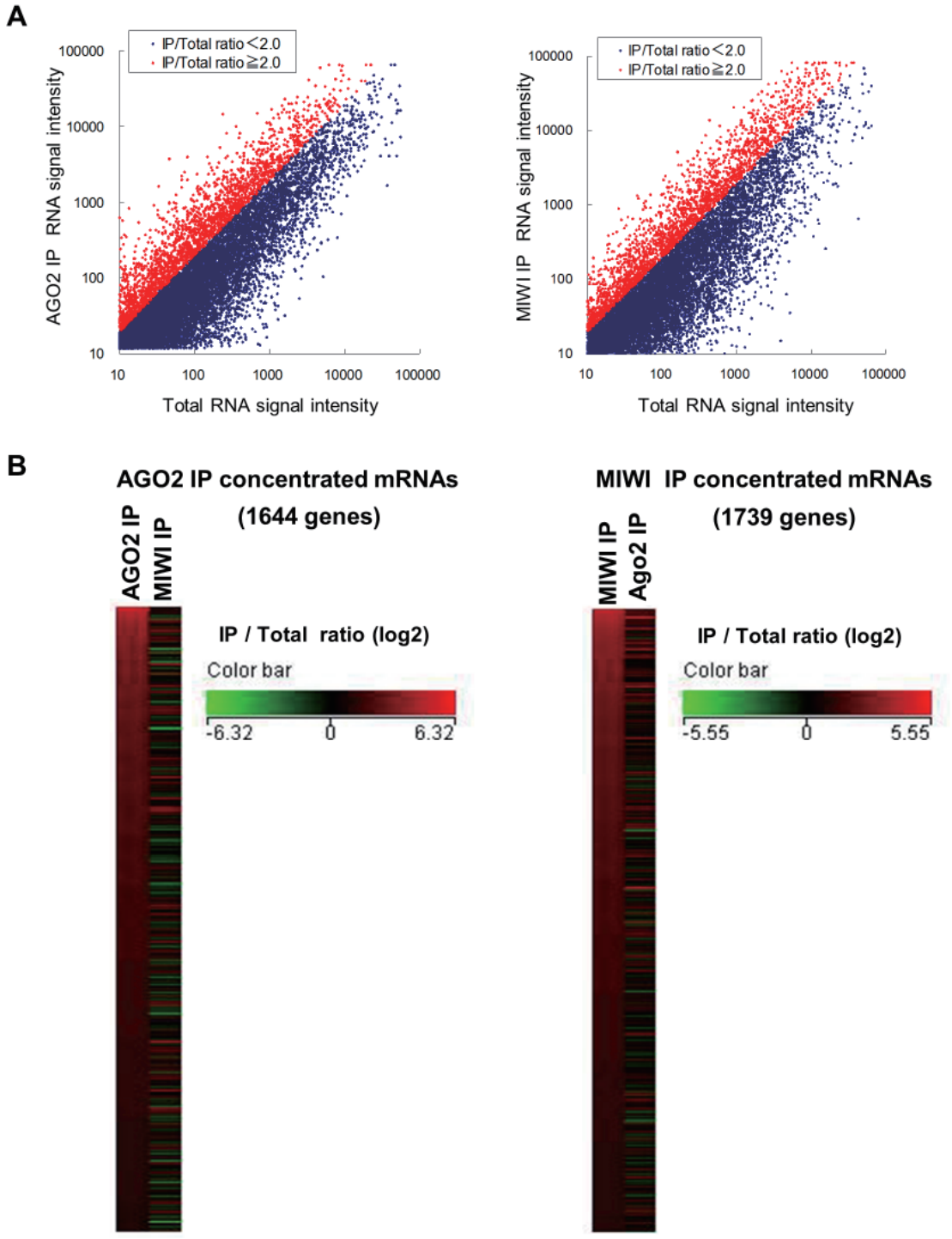


**Figure 4. Microarray analysis of mRNAs contained in the MIWI complex. (A)** Scatter plot of signal intensity ($log_{10}$) between AGO2-IP RNA and total RNA (left) and between MIWI-IP RNA and total RNA (right). Total RNA, AGO2-IP RNA and MIWI-IP RNA were isolated from adult testes. Total RNA labeled with Cy3 and AGO2-IP RNA or MIWI-IP RNA labeled with Cy5 were hybridized onto a 3D-Gene® Mouse Oligo chip 25k. The signals for which the IP RNA/total RNA signal ratio was ≥ 2.0 are shown in red, and those for signal ratio < 2.0 are shown in blue. **(B)** Heat map of the ratio of signal intensities of AGO2-IP RNA to total RNA and MIWI-IP RNA to total RNA. We selected 1644 (left) and 1739 (right) mRNAs as enriched mRNA in the AGO2-IP products and the MIWI-IP products, respectively, based on the signal ratio of the IP RNA to total RNA ≥ 2.0, and compared the ratio ($log_2$) of signal intensities of AGO2-IP RNA to total RNA and MIWI-IP RNA to total RNA.

Interestingly, we found that *Aym1* mRNA, encoding not only a protein but also several piRNAs, was included among the mRNAs highly and specifically enriched in the MIWI-IP products (Figure S6). One of the piRNAs specifically encoded in *Aym1* mRNA, piR-18928, was generated in the testes and its expression level increased from 12-20 dpp, similarly to *Aym1* mRNA (Figures S7A and S7B). AYM1 protein has been reported to be expressed in pachytene spermatocytes (*39*). In pachytene spermatocytes, the

**Table 2. Expression analysis of mRNAs highly and specifically enriched in the MIWI-IP products during spermatogenesis**

| Category | Gene symbol | Microarray signal ratio | | Relative mRNA level (20 dpp/12 dpp) |
|---|---|---|---|---|
| | | AGO2-IP/Total | MIWI-IP/Total | |
| AGO2-IP | *Gca* | 26.8 | 0.1 | 0.2 |
| | *Rgs2* | 21.7 | 0.2 | 0.6 |
| | *Cmpk* | 20.1 | 0.5 | 1.1 |
| | *Btg3* | 17.7 | 0.2 | 1.2 |
| | *Reep1* | 15.7 | 0.2 | 1.2 |
| | *Cdc42se2* | 14.9 | 0.2 | 1.0 |
| | *8430410K20Rik* | 14.2 | 0.3 | 1.3 |
| | *Myadm* | 13.1 | 0.8 | 0.8 |
| | *Rnf11* | 12.3 | 0.3 | 1.1 |
| | *Mex3c* | 12.3 | 1.1 | 1.1 |
| | Mean | 16.9 | 0.4 | 1.0 |
| MIWI-IP | *Dynlrb2* | 1.2 | 22.5 | 61.9 |
| | *Aym1* | 0.4 | 19.6 | 39.8 |
| | *Mrps18c* | 1.1 | 18.8 | 3.1 |
| | *Chchd1* | 1.3 | 17.6 | 3.8 |
| | *Bcmo1* | 0.5 | 16.4 | 13.3 |
| | *H2-DMb2* | 1.3 | 15.8 | 1.9 |
| | *Ddt* | 0.9 | 15.5 | 9.1 |
| | *Wfdc15* | 1.4 | 14.7 | 14.8 |
| | *Rpp21* | 1.2 | 11.8 | 8.9 |
| | *Cdk5rap1* | 0.9 | 11.3 | 2.5 |
| | Mean | 1.0 | 16.4 | 15.9 |

The expression levels of the top ten mRNAs each, highly and specifically enriched in the AGO2-IP and MIWI-IP products, were analyzed by quantitative PCR in mouse testes at 12 and 20 dpp, and normalized to those of Gapdh. The normalized levels at 20 dpp were compared with those at 12 dpp. dpp, days postpartum.

**Table 3. Pathway analysis of mRNAs enriched in the MIWI-IP products**

| Category | MAPP name | # measured | # on MAPP | % changed | % present | Z score |
|---|---|---|---|---|---|---|
| AGO2-IP | mRNA_processing_binding_Reactome | 378 | 551 | 19 | 69 | 4.0 |
| | Methionine_metabolism | 6 | 26 | 50 | 23 | 2.8 |
| | Circadian_Exercise | 42 | 49 | 26 | 86 | 2.7 |
| | Electron_Transport_Chain | 63 | 83 | 22 | 76 | 2.3 |
| | 2_4_Dichlorobenzoate_degradation | 4 | 32 | 50 | 13 | 2.3 |
| | RNA_transcription_Reactome | 38 | 41 | 24 | 93 | 2.1 |
| MIWI-IP | Electron_Transport_Chain | 63 | 83 | 51 | 76 | 10.2 |
| | Ribosomal_Proteins | 49 | 80 | 35 | 61 | 5.4 |
| | mRNA_processing_binding_Reactome | 378 | 551 | 16 | 69 | 3.1 |
| | RNA_transcription_Reactome | 38 | 41 | 26 | 93 | 3.1 |
| | Hedgehog_Netpath_10 | 21 | 21 | 29 | 100 | 2.6 |
| | Small_ligand_GPCRs | 19 | 19 | 26 | 100 | 2.2 |
| | Biotin_metabolism | 5 | 13 | 40 | 38 | 2.1 |

1,644 and 1,739 mRNAs were selected as enriched mRNA in the AGO2-IP and MIWI-IP products, respectively, based on the signal ratio of the IP RNA to total RNA ≥ 2.0 by microarray expression analysis. These mRNAs were applied to the GenMAPP pathway profiler. The pathways for which the Z score was above 2.0 are listed in the table. From the left-hand side the columns indicate: category; the name of the pathway (MAPP name); the number of mRNAs for which the IP RNA/total RNA signal ratio was ≥ 2.0 (# changed); the number of mRNAs used for the analysis (# measured); the number of mRNAs in the pathway (# on MAPP); the percentage of the number changed per the number measured (% changed); the percentage of the number measured per the number on MAPP (% present); and the Z-score.

*Aym1* mRNA appears to generate both the AYM1 protein and the piRNA. Furthermore, piR-18928 was undetectable in *Miwi*$^{-/-}$ testes, whereas *Aym1* mRNA did not show such a reduction in *Miwi*$^{-/-}$ testes (Figures S7C and S7D). These results suggest that MIWI is also involved in pachytene piRNA biogenesis from mRNA-type piRNA precursor.

In addition, mRNAs encoding electron transport chain, ribosomal and mitochondrial ribosomal proteins were present specifically in the MIWI-IP products (Table 3). This result indicates that MIWI associates with many mRNAs encoding mitochondrial proteins. Since the expression levels of these mRNAs at 20 dpp were higher than that at 12 dpp (Table S2), the expression level of these mRNAs also tends to increase in pachytene spermatocytes.

**Table 4. Expression analysis of mRNAs highly and specifically enriched in the MIWI-IP products in Miwi-deficient testes**

| Category | Gene symbol | Relative mRNA level (*Miwi*$^{-/-}$/*Miwi*$^{+/-}$) | | |
|---|---|---|---|---|
| | | 20 dpp | 22 dpp | 24 dpp |
| AGO2-IP | *Gca* | 1.10 | 1.17 | 0.97 |
| | *Rgs2* | 1.25 | 1.08 | 1.17 |
| | *Cmpk* | 1.00 | 1.05 | 1.18 |
| | *Btg3* | 0.95 | 0.99 | 1.15 |
| | *Reep1* | 0.92 | 1.02 | 0.90 |
| | *Cdc42se2* | 0.95 | 0.96 | 0.98 |
| | *8430410K20Rik* | 0.93 | 1.08 | 1.08 |
| | *Myadm* | 1.08 | 0.81 | 0.96 |
| | *Rnf11* | 0.91 | 0.95 | 1.03 |
| | *Mex3c* | 0.95 | 0.95 | 0.82 |
| | Mean | 1.01 | 1.01 | 1.02 |
| MIWI-IP | *Dynlrb2* | 0.64 | 0.96 | 1.15 |
| | *Aym1* | 0.82 | 1.13 | 1.37 |
| | *Mrps18c* | 0.88 | 1.04 | 1.14 |
| | *Chchd1* | 0.72 | 1.02 | 1.16 |
| | *Bcmo1* | 0.51 | 0.82 | 0.64 |
| | *H2-DMb2* | 0.68 | 1.16 | 1.00 |
| | *Ddt* | 0.62 | 0.89 | 1.02 |
| | *Wfdc15* | 0.67 | 0.85 | 0.97 |
| | *Rpp21* | 0.74 | 0.87 | 1.04 |
| | *Cdk5rap1* | 0.75 | 0.85 | 0.97 |
| | Mean | 0.70 | 0.96 | 1.05 |

The expression levels of ten mRNAs each, highly and specifically enriched in the AGO2-IP products and the MIWI-IP products, were analyzed by quantitative PCR in *Miwi*$^{+/-}$ and *Miwi*$^{-/-}$ testes at 20, 22 and 24 dpp, and normalized to those of Gapdh. The normalized levels in *Miwi*$^{-/-}$ testes were compared with those in *Miwi*$^{+/-}$ testes. dpp, days postpartum.

### 3.6. *Expression of mRNAs enriched in the MIWI-IP products is decreased in Miwi-deficient testes*

We compared the expression levels of the top ten mRNAs that were highly and specifically enriched in the AGO2-IP and MIWI-IP products in *Miwi*$^{+/-}$ and *Miwi*$^{-/-}$ mice testes at 20, 22, and 24 dpp. mRNAs enriched in the MIWI-IP products were decreased by 20-30% in 20 dpp *Miwi*$^{-/-}$ testes, although these mRNAs did not show a significant reduction in RNA levels at 22 or 24 dpp (Table 4). In contrast, mRNAs enriched in the AGO2-IP products did not show such a reduction in *Miwi*$^{-/-}$ testes. We also performed a similar analysis of mRNAs encoding electron transport chain and ribosomal proteins enriched in MIWI-IP products, and these mRNA levels were decreased by approximately 20% in 20 dpp *Miwi*$^{-/-}$ testes (Table S3). These results indicated that at 20 dpp, *Miwi*$^{-/-}$ testes have reduced MIWI-associated mRNAs, specifically when pachytene spermatocytes are most abundant. We also compared the RNA and protein levels of two mRNAs highly enriched in the MIWI-IP products, *Ssna1* and *Nasp*, in *Miwi*$^{+/-}$ and *Miwi*$^{-/-}$ testes at 20, 22 and 24 dpp. The protein abundance ratio of these mRNAs in *Miwi*$^{+/-}$ and *Miwi*$^{-/-}$ testes correlated approximately with the RNA abundance ratio (Figure S8). These results suggest that MIWI is involved in stabilization of target mRNAs rather than translational regulation in pachytene spermatocytes.

## 4. Discussion

Since *Miwi*$^{-/-}$ mice display spermatogenic arrest at the round spermatid stage, MIWI has been thought to play an essential role in spermiogenesis (*10*). Recently, analysis of *Miwi*$^{-/-}$/*Miwi*$^{-/-}$ double knockout mice revealed that PIWI proteins including MIWI are required for spermatogenesis (*40*). However, the function of MIWI in spermatogenesis and spermiogenesis is not well understood. In this study, we investigated MIWI-associated poly(A) RNAs, and revealed that MIWI may play an important role in piRNA biogenesis and target mRNA metabolism in pachytene spermatocytes before spermiogenesis.

### 4.1. *MIWI may be directly involved in pachytene piRNA biogenesis*

The biogenesis of piRNAs is independent of Dicer in flies and zebrafish, and thus it is thought that piRNAs are generated from single-stranded RNA precursors (*41,42*). In mice, long precursor RNAs of piRNA-like RNAs, moderately long precursor RNAs of piRNAs and mRNA-type piRNA precursors were identified (*43-46*). However, it is still unclear whether MIWI is involved in processing of these precursor RNAs. In this study, we show that MIWI associates with non-coding type piRNA precursors, such as clone No. 5, and mRNA-type piRNA precursor, such as *Aym1* mRNA

(Figure 2D and Table 2). The expression level of these piRNA-encoding RNAs was increased in pachytene spermatocytes (Figures 3A and S7A), and mature piRNAs specifically encoded in these piRNA-encoding RNAs were generated in pachytene spermatocytes (Figures 3B and S7B). Moreover, *Miwi*$^{-/-}$ testes did not generate these mature piRNAs (Figures 3C and S7C). Therefore, we conclude that these RNAs are pachytene piRNA precursors, and that MIWI may be involved in processing of these piRNA precursor RNAs. Most recently, the study of MIWI-catalytic activity mutant mice revealed that the slicer activity of MIWI is not required for piRNA biogenesis (*27*). Hence, not only MIWI but also other factors appear to be required for processing of pachytene piRNA precursors, and further study is required to identify these factors.

4.2. *MIWI may play an important role in the positive regulation of target mRNAs in pachytene spermatocytes*

In both the MIWI-IP and AGO2-IP products, approximately 70% of poly(A) RNAs encoded known mRNAs (Figure 2B). We compared the mRNA species enriched in the MIWI and AGO2 complexes by microarray analysis. Many mRNA species whose expression level was increased in pachytene spermatocytes were specifically enriched in the MIWI-IP products (Table 2). This result suggests that MIWI may target mRNAs that play important roles in pachytene spermatocytes. In particular, those mRNAs encoding mitochondrial proteins, likely electron transport chain and mitochondrial ribosomal proteins, were enriched in the MIWI-IP products (Table 3). Previous reports show that mitochondrial function is essential for meiosis in yeast and mouse testes (*47,48*). Furthermore, the mitochondrial membrane protein MITOPLD is essential for nuage formation and piRNA biogenesis, indicating that mitochondrial function is closely related to piRNA biogenesis (*49,50*). The possibility that MIWI targets a large number of mRNA species encoding mitochondrial proteins provides new insight into MIWI function.

Finally, we investigated the possibility that MIWI is involved in post-transcriptional regulation of target mRNAs. We compared the RNA level of mRNAs enriched in the MIWI-IP products in *Miwi*$^{+/-}$ and *Miwi*$^{-/-}$ testes. These mRNAs were decreased by 20-30% in 20 dpp *Miwi*$^{-/-}$ testes, but did not show any significant reduction at 22 or 24 dpp (Table 4 and S3). Pachytene spermatocytes have high levels of MIWI-associated mRNAs. Therefore, the reduction of MIWI-associated mRNAs in *Miwi*$^{-/-}$ testes at 20 dpp, when pachytene spermatocytes are most abundant, suggests that MIWI is involved in mRNA stabilization in these cells. There remains a possibility that delayed differentiation of pachytene spermatocytes could lead to a significant reduction in RNA levels in 20 dpp *Miwi*$^{-/-}$ testes. Hence, further study is required to compare mRNA levels in pachytene spermatocytes isolated from *Miwi*$^{+/-}$ and *Miwi*$^{-/-}$ testes. Furthermore, in this study we could not clarify whether piRNAs mediate MIWI binding to its target mRNA. Future studies are also needed to elucidate whether MIWI associates with mRNAs in a piRNA mediated manner.

**Acknowledgements**

We thank Dr. H. Lin (Yale University) for providing *Miwi* knockout mice, and Hideo Akiyama and Satoshi Kondo (Toray Industries, Inc.) for supporting the microarray analysis. We also thank Takahisa Kobayashi for supporting production of monoclonal antibodies, and Masaki Warashina, Makoto Amano, Taku Funakoshi, and Hitoshi Uemori for valuable discussions and advice.

**References**

1. Sasaki T, Shiohama A, Minoshima S, Shimizu N. Identification of eight members of the Argonaute family in the human genome small star, filled. Genomics. 2003; 82:323-330.
2. Liu J, Carmell MA, Rivas FV, Marsden CG, Thomson JM, Song JJ, Hammond SM, Joshua-Tor L, Hannon GJ. Argonaute2 is the catalytic engine of mammalian RNAi. Science. 2004; 305:1437-1441.
3. Meister G, Landthaler M, Patkaniowska A, Dorsett Y, Teng G, Tuschl T. Human Argonaute2 mediates RNA cleavage targeted by miRNAs and siRNAs. Mol Cell. 2004; 15:185-197.
4. Pillai RS, Artus CG, Filipowicz W. Tethering of human Ago proteins to mRNA mimics the miRNA-mediated repression of protein synthesis. RNA. 2004; 10:1518-1525.
5. Aravin A, Gaidatzis D, Pfeffer S, *et al.* A novel class of small RNAs bind to MILI protein in mouse testes. Nature. 2006; 442:203-207.
6. Girard A, Sachidanandam R, Hannon GJ, Carmell MA. A germline-specific class of small RNAs binds mammalian Piwi proteins. Nature. 2006; 442:199-202.
7. Grivna ST, Beyret E, Wang Z, Lin H. A novel class of small RNAs in mouse spermatogenic cells. Genes Dev. 2006; 20:1709-1714.
8. Lau NC, Seto AG, Kim J, Kuramochi-Miyagawa S, Nakano T, Bartel DP, Kingston RE. Characterization of the piRNA complex from rat testes. Science. 2006; 313:363-367.
9. Watanabe T, Takeda A, Tsukiyama T, Mise K, Okuno T, Sasaki H, Minami N, Imai H. Identification and characterization of two novel classes of small RNAs in the mouse germline: Retrotransposon-derived siRNAs in oocytes and germline small RNAs in testes. Genes Dev. 2006; 20:1732-1743.
10. Deng W, Lin H. *Miwi*, a murine homolog of piwi, encodes a cytoplasmic protein essential for spermatogenesis. Dev Cell. 2002; 2:819-830.
11. Kuramochi-Miyagawa S, Kimura T, Ijiri TW, Isobe T, Asada N, Fujita Y, Ikawa M, Iwai N, Okabe M, Deng W, Lin H, Matsuda Y, Nakano T. *Mili*, a mammalian member

of piwi family gene, is essential for spermatogenesis. Development. 2004; 131:839-849.
12. Carmell MA, Girard A, van de Kant HJ, Bourc'his D, Bestor TH, de Rooij DG, Hannon GJ. MIWI2 is essential for spermatogenesis and repression of transposons in the mouse male germline. Dev Cell. 2007; 12:503-514.
13. Aravin AA, Sachidanandam R, Bourc'his D, Schaefer C, Pezic D, Toth KF, Bestor T, Hannon GJ. A piRNA pathway primed by individual transposons is linked to *de novo* DNA methylation in mice. Mol Cell. 2008; 31:785-799.
14. Unhavaithaya Y, Hao Y, Beyret E, Yin H, Kuramochi-Miyagawa S, Nakano T, Lin H. MILI, a PIWI-interacting RNA-binding protein, is required for germ line stem cell self-renewal and appears to positively regulate translation. J Biol Chem. 2009; 284:6507-6519.
15. Kuramochi-Miyagawa S, Watanabe T, Gotoh K, *et al.* DNA methylation of retrotransposon genes is regulated by Piwi family members MILI and MIWI2 in murine fetal testes. Genes Dev. 2008; 22:908-917.
16. Aravin AA, Sachidanandam R, Girard A, Fejes-Toth K, Hannon GJ. Developmentally regulated piRNA clusters implicate MILI in transposon control. Science. 2007; 316:744-747.
17. Kojima K, Kuramochi-Miyagawa S, Chuma S, Tanaka T, Nakatsuji N, Kimura T, Nakano T. Associations between PIWI proteins and TDRD1/MTR-1 are critical for integrated subcellular localization in murine male germ cells. Genes Cells. 2009; 14:1155-1165.
18. Reuter M, Chuma S, Tanaka T, Franz T, Stark A, Pillai RS. Loss of the Mili-interacting Tudor domain-containing protein-1 activates transposons and alters the Mili-associated small RNA profile. Nat Struct Mol Biol. 2009; 16:639-646.
19. Shoji M, Tanaka T, Hosokawa M, *et al.* The TDRD9-MIWI2 complex is essential for piRNA-mediated retrotransposon silencing in the mouse male germline. Dev Cell. 2009; 17:775-787.
20. Vagin VV, Wohlschlegel J, Qu J, Jonsson Z, Huang X, Chuma S, Girard A, Sachidanandam R, Hannon GJ, Aravin AA. Proteomic analysis of murine Piwi proteins reveals a role for arginine methylation in specifying interaction with Tudor family members. Genes Dev. 2009; 23:1749-1762.
21. Wang J, Saxe JP, Tanaka T, Chuma S, Lin H. Mili interacts with tudor domain-containing protein 1 in regulating spermatogenesis. Curr Biol. 2009; 19:640-644.
22. Frost RJ, Hamra FK, Richardson JA, Qi X, Bassel-Duby R, Olson EN. MOV10L1 is necessary for protection of spermatocytes against retrotransposons by Piwi-interacting RNAs. Proc Natl Acad Sci U S A. 2010; 107:11847-11852.
23. Kuramochi-Miyagawa S, Watanabe T, Gotoh K, *et al*. MVH in piRNA processing and gene silencing of retrotransposons. Genes Dev. 2010; 24:887-892.
24. Zheng K, Xiol J, Reuter M, Eckardt S, Leu NA, McLaughlin KJ, Stark A, Sachidanandam R, Pillai RS, Wang PJ. Mouse MOV10L1 associates with Piwi proteins and is an essential component of the Piwi-interacting RNA (piRNA) pathway. Proc Natl Acad Sci U S A. 2010; 107:11841-11846.
25. Chi YH, Cheng LI, Myers T, Ward JM, Williams E, Su Q, Faucette L, Wang JY,Jeang KT. Requirement for Sun1 in the expression of meiotic reproductive genes and piRNA. Development. 2009; 136:965-973.
26. Ma L, Buchold GM, Greenbaum MP, Roy A, Burns KH, Zhu H, Han DY, Harris RA, Coarfa C, Gunaratne PH, Yan W, Matzuk MM. GASZ is essential for male meiosis and suppression of retrotransposon expression in the male germline. PLoS Genet. 2009; 5:e1000635.
27. Reuter M, Berninger P, Chuma S, Shah H, Hosokawa M, Funaya C, Antony C, Sachidanandam R, Pillai RS. Miwi catalysis is required for piRNA amplification-independent LINE1 transposon silencing. Nature. 2011; 480:264-267.
28. Kotaja N, Bhattacharyya SN, Jaskiewicz L, Kimmins S, Parvinen M, Filipowicz W,Sassone-Corsi P. The chromatoid body of male germ cells: Similarity with processing bodies and presence of Dicer and microRNA pathway components. Proc Natl Acad Sci U S A. 2006; 103:2647-2652.
29. Grivna ST, Pyhtila B, Lin H. MIWI associates with translational machinery and PIWI-interacting RNAs (piRNAs) in regulating spermatogenesis. Proc Natl Acad Sci U S A. 2006; 103:13415-13420.
30. Hayashi K, Chuva de Sousa Lopes SM, Kaneda M, Tang F, Hajkova P, Lao K, O'Carroll D, Das PP, Tarakhovsky A, Miska EA,Surani MA. MicroRNA biogenesis is required for mouse primordial germ cell development and spermatogenesis. PLoS One. 2008; 3:e1738.
31. Hayashida Y, Nishibu T, Inoue K,Kurokawa T. A useful approach to total analysis of RISC-associated RNA. BMC Res Notes. 2009; 2:169.
32. Iwasaki S, Kobayashi M, Yoda M, Sakaguchi Y, Katsuma S, Suzuki T, Tomari Y. Hsc70/Hsp90 chaperone machinery mediates ATP-dependent RISC loading of small RNA duplexes. Mol Cell. 2010; 39:292-299.
33. Brennecke J, Aravin AA, Stark A, Dus M, Kellis M, Sachidanandam R, Hannon GJ. Discrete small RNA-generating loci as master regulators of transposon activity in Drosophila. Cell. 2007; 128:1089-1103.
34. Gunawardane LS, Saito K, Nishida KM, Miyoshi K, Kawamura Y, Nagami T, Siomi H, Siomi MC. A slicer-mediated mechanism for repeat-associated siRNA 5' end formation in Drosophila. Science. 2007; 315:1587-1590.
35. Bellve AR. Purification, culture, and fractionation of spermatogenic cells. Methods Enzymol. 1993; 225:84-113.
36. Liu D, Matzuk MM, Sung WK, Guo Q, Wang P, Wolgemuth DJ. Cyclin A1 is required for meiosis in the male mouse. Nat Genet. 1998; 20:377-380.
37. Kawamata M, Nishimori K. Mice deficient in Dmrt7 show infertility with spermatogenic arrest at pachytene stage. FEBS Lett. 2006; 580:6442-6446.
38. Li B, Nair M, Mackay DR, Bilanchone V, Hu M, Fallahi M, Song H, Dai Q, Cohen PE, Dai X. Ovol1 regulates meiotic pachytene progression during spermatogenesis by repressing Id2 expression. Development. 2005; 132:1463-1473.
39. Malcov M, Cesarkas K, Stelzer G, Shalom S, Dicken Y, Naor Y, Goldstein RS, Sagee S, Kassir Y, Don J. *Aym1*, a mouse meiotic gene identified by virtue of its ability to activate early meiotic genes in the yeast Saccharomyces cerevisiae. Dev Biol. 2004; 276:111-123.
40. Beyret E, Lin H. Pinpointing the expression of piRNAs and function of the PIWI protein subfamily during spermatogenesis in the mouse. Dev Biol. 2011; 355:215-226.
41. Vagin VV, Sigova A, Li C, Seitz H, Gvozdev V, Zamore

PD. A distinct small RNA pathway silences selfish genetic elements in the germline. Science. 2006; 313:320-324.
42. Houwing S, Kamminga LM, Berezikov E, Cronembold D, Girard A, van den Elst H, Filippov DV, Blaser H, Raz E, Moens CB, Plasterk RH, Hannon GJ, Draper BW, Ketting RF. A role for Piwi and piRNAs in germ cell maintenance and transposon silencing in Zebrafish. Cell. 2007; 129:69-82.
43. Iguchi N, Xu M, Hori T, Hecht NB. Noncoding RNAs of the mammalian testis: The meiotic transcripts Nct1 and Nct2 encode piRNAs. Ann N Y Acad Sci. 2007; 1120:84-94.
44. Ro S, Park C, Song R, Nguyen D, Jin J, Sanders KM, McCarrey JR, Yan W. Cloning and expression profiling of testis-expressed piRNA-like RNAs. RNA. 2007; 13:1693-1702.
45. Xu M, You Y, Hunsicker P, Hori T, Small C, Griswold MD, Hecht NB. Mice deficient for a small cluster of Piwi-interacting RNAs implicate Piwi-interacting RNAs in transposon control. Biol Reprod. 2008; 79:51-57.
46. Robine N, Lau NC, Balla S, Jin Z, Okamura K, Kuramochi-Miyagawa S, Blower MD, Lai EC. A broadly conserved pathway generates 3'UTR-directed primary piRNAs. Curr Biol. 2009; 19:2066-2076.
47. Nakada K, Sato A, Yoshida K, Morita T, Tanaka H, Inoue S, Yonekawa H,Hayashi J. Mitochondria-related male infertility. Proc Natl Acad Sci U S A. 2006; 103:15148-15153.
48. Treinin M,Simchen G. Mitochondrial activity is required for the expression of IME1, a regulator of meiosis in yeast. Curr Genet. 1993; 23:223-227.
49. Huang H, Gao Q, Peng X, Choi SY, Sarma K, Ren H, Morris AJ, Frohman MA. piRNA-associated germline nuage formation and spermatogenesis require MitoPLD profusogenic mitochondrial-surface lipid signaling. Dev Cell. 2011; 20:376-387.
50. Watanabe T, Chuma S, Yamamoto Y, Kuramochi-Miyagawa S, Totoki Y, Toyoda A, Hoki Y, Fujiyama A, Shibata T, Sado T, Noce T, Nakano T, Nakatsuji N, Lin H, Sasaki H. MITOPLD is a mitochondrial protein essential for nuage formation and piRNA biogenesis in the mouse germline. Dev Cell. 2011; 20:364-375.

(*Received May 9, 2012; Revised August 30, 2012; Accepted September 14, 2012*)